Acta Mech 233, 437–453 (2022)
https://doi.org/10.1007/s00707-021-03105-2

ORIGINAL PAPER

Stephen Kirwa Melly · Liwu Liu · Yanju Liu · Jinsong Leng

Modified Yeoh model with improved equibiaxial loading predictions

Received: 14 July 2021 / Revised: 24 September 2021 / Accepted: 27 October 2021 / Published online: 22 January 2022

Abstract Based on two sets of experimental data from the literature, one for vulcanized rubber and the other for a thermoplastic elastomer, the Yeoh model was found to underestimate the stress during equibiaxial loading. The Biderman model, whose strain energy density function expression differs from that of the Yeoh model by an additional term containing the second invariant, overestimates the stress in the mentioned loading mode leading to severe inaccuracies. For improved predictions, this work proposes the modification of the Yeoh model in which the residual strain energy density from equibiaxial loading is fitted to a term with dependence on the second invariant and thereafter adding the term to the original expression. The model constants and predictions were obtained by implementing the Levenberg–Marquardt algorithm and the Cauchy stress tensor equations, respectively, in Python codes. Both the coefficient of determination and the relative errors were utilized to quantify the accuracy of the model predictions. The modified model exhibited superior predictive capabilities particularly in equibiaxial loading where it reduced the average relative error from 22.07 to 6.09 and 27.25 to 10.39% for vulcanized rubber and thermoplastic elastomer data, respectively. For complete behavior, i.e., the average of the relative errors in the three loading modes, the modified version's value was half that of the Yeoh model. This demonstrated its suitability for predicting the multi-axial loading behavior of elastomer-based engineering components.

1 Introduction

When subjected to loading conditions, elastomeric materials are known to exhibit a characteristically complex mechanical behavior that involves both geometric and material nonlinearities in that extremely large shape changes occur and the stress–strain relation is highly nonlinear. Importantly, the large nonlinear deformation is ideally elastic meaning that it is recoverable upon the removal of the load. It is for this reason that materials with such behavior are termed *hyperelastic* or *Green elastic*. In addition to the mechanical behavior mentioned, elastomeric materials are intrinsically resistant to abrasion, excellent thermal and electrical insulators, and durable, thus find extensive applications in engineering industries such as aerospace and automotive [1]. Before the fabrication of an elastomeric component, a design process that necessitates a proper understanding of the mechanical behavior of the material must be meticulously executed. The key to a successful design is a constitutive model that accurately describes the stress–strain relation under various loading conditions. The

S. K. Melly · L. Liu (✉) · Y. Liu
Department of Astronautical Science and Mechanics, Harbin Institute of Technology (HIT), No. 92 West Dazhi Street, P.O. Box 301, Harbin 150001, People's Republic of China
e-mail: liuliwu_006@163.com

J. Leng (✉)
Center for Composite Materials and Structures, Harbin Institute of Technology (HIT), No. 2 Yikuang Street, P.O. Box 3011, Harbin 150080, People's Republic of China
e-mail: lengjs@hit.edu.cn

tremendous advances in the computational capabilities of computers, the availability of finite element analysis (FEA) programs, and the development of accurate constitutive models has enabled the three-dimensional analysis of engineering components with complex geometry and loading conditions an easy task. Computational modeling is nowadays essential during the design of engineering components. As such, the research on developing models that accurately predict the material behavior under any loading condition remains an active and crucial undertaking for optimized engineering designs.

The nonlinear stress–strain relation renders Hooke's law invalid in predicting the material's response to loading [2]. Therefore, the formulation of Cauchy stress expression for nonlinearly elastic materials is based on a function that is commonly known as strain energy density (W). It represents the work done per unit volume of the material in the undeformed configuration to deform it to the current configuration [3]. The form of W is determined based on two different approaches, namely phenomenological and micromechanical. The former employs continuum mechanics techniques that result in mathematical equations that are dependent on strain invariants or principal stretches whereas the latter utilizes statistical mechanics to describe the material response from the microstructure level. There have been attempts to develop hybrid models that utilize both of the approaches mentioned [4]. In both cases, there are several mathematical restrictions imposed on W that have physical meanings, e.g., it should yield zero value at the undeformed state [5]. The phenomenological models are more popular in the literature and for practical use thanks to their model parameters that are easily obtained by fitting experimental data. Classical phenomenological-based models that are frequently referenced in the literature and are incorporated into some of the finite element programs include neo-Hookean [6], Mooney-Rivlin [7], Yeoh [8, 9], Ogden [10], and Gent [11]. On the other hand, well-known micromechanical-based models include eight-chain by Arruda and Boyce [12], and the extended tube model [13]. It is worth noting that the neo-Hookean model can be derived from both approaches. More recent models include Carroll [14], Anssari-Benam and Bucchi [15], Yaya and Bechir [16], Mansouri and Darijani [17], Khajehsaeid et al. [18], Zhao et al. [19], Kaoye et al. [20], and Külcü [21]. For engineers to make informed decisions on the right models to use in their designs, some authors have presented the comparative performance of various models. These include the work of Marckmann and Verron [22] who did a comparison study on twenty hyperelastic models based on how each could reproduce two sets of classical experimental data, the recent work of Fujikawa et al. [23] wherein the performances of four models were compared with a focus on their predictive capabilities in multi-axial loading when model parameters are obtained from a single test, and an earlier work by Seibert and Schöche [24].

The loading subjected to an engineering component in practical application is complex and involves multi-axial deformation modes. Therefore, the experimental data from three individual loading modes, namely uniaxial tension, equibiaxial extension, and pure shear, are normally utilized in benchmarking the predictive capabilities of new models. A reliable model that can describe the response under general deformation should be able to accurately predict the experimental behavior in each of the mentioned loading modes. Furthermore, it should require only a single set of model constants and should apply to a wide variety of materials. It is more desirable if the single set of parameters can be determined from a single set of experimental data such as uniaxial tension loading. This reduces the number of experiments required to calibrate the model as opposed to models requiring the simultaneous fitting of experimental data from different loading modes. It is quite challenging to realize a model with all the mentioned characteristics. As such, researchers are continuously motivated to develop new models or modify the existing ones for improved performances. For instance, the eight-chain model [12] describes the uniaxial and pure shear loadings very well but is known to unsatisfactorily predict the equibiaxial tension. Hossain et al. [25] presented modified versions of this model that have better predictions in EB. The Gent model [11] is a modified version of the neo-Hookean model [6] and it performs somewhat better than the latter. Hohenberger et al. [26] modified the Yeoh model to capture the large strain nonlinearities in highly filled elastomers. The recent work by Melly et al. [27] modified the Carroll model [14] so that its W vanishes at the reference configuration and includes a compressibility term. Their resultant model was advantageous in that material parameters could be obtained in a single fitting, recorded better predictive performance, and could be implemented in a finite element program. One of the complex nonlinear features of the stress–strain behavior of elastomeric materials is the strain-stiffening effect whereby the stress rapidly increases at the strain limit. For realistic finite element simulations of elastomeric component deformation and damage, the constitutive equation should not only capture the strain-stiffening effect but also bound the strain energy so that it does not grow to infinity, and the stress should also be bounded to asymptotically vanish with increasing strain up to failure. The authors [28, 29] proposed direct, explicit, and straightforward approaches to formulate the W expression that matches the experimental data, describes the strain-stiffening effect, and bounds the strain energy so that it never grows to infinity. In their subsequent work [30], the authors included the capability of the model to estimate errors in any deformation mode.

The relative advantages of the Yeoh model [9] include a simply expressed W, few material parameters, a single set of model constants are required for all deformation modes, the constants are obtained by fitting only the uniaxial tension data, and works well for a variety of materials under large deformation range. Consequently, it is frequently employed in analyzing the response of hyperelastic materials. Gajewski et al. [31] simulated the behavior of elastomeric bearings under loading conditions by utilizing the Yeoh model in an FE program. Renaud et al. [32] applied the Yeoh model in an FE program to study the large deformation of a hyperelastic body under contact/impact loadings. Recently, Jaramillo [33] found the Yeoh model to better predict the behavior of biological tissue (Annulus Fibrosus). The very recent work of Forsat [34] studied the suitability of several hyperelastic models including the Yeoh model in modeling the nonlinear vibration of hyperelastic beams. Despite the numerous advantages and wide applicability, Yeoh's model prediction in equibiaxial tension is to relatively lower accuracy and may deviate significantly for different materials. As such, it may predict inaccurately in the case of multi-axial loading. This behavior is not a surprise as the W expression for the Yeoh model is only dependent on the first invariant. W expressions with sole dependence on the first invariant have been found to unsatisfactorily predict equibiaxial tension loading behavior [35]. It has been proven that the inclusion of the second invariant leads to more accurate predictions specifically in the equibiaxial tension [36].

In this work, the W expression for the Yeoh model is modified for enhanced predictions particularly in the equibiaxial loading mode by adding a single term involving the second invariant. The process of adding the term follows the work of Carroll [14] in which the W expression is derived by following systematic steps of fitting the strain energy density of the residual stress to an equation that is dependent on either the first or the second invariant. In this case, the residual stress is the difference between the predicted and the experimental stress data in a specific loading mode. Firstly, based on the classical experimental data of Treloar [37] (8% S vulcanized rubber) and the recent data due to Zhao [38] (Entec Enflex S4035A thermoplastic elastomer, TPE), the Biderman [39] and the Yeoh models are demonstrated to inaccurately capture the behavior in equibiaxial loading. The difference between the W expressions for the two models is that the former contains an additional term that is dependent on the second invariant. Secondly, the strain energy density of the residual stress in equibiaxial tension is calculated and then fitted to a term involving the second invariant. The W expression for the Yeoh model is then modified by adding the term. Lastly, the predictive capabilities of the modified version are then compared with those of the original version.

2 Basic equations

2.1 Description of large deformation

In large deformation theory, the coordinates of a material point in the undeformed and deformed configurations are represented by $\mathbf{X}$ and $\mathbf{x}$, respectively. The deformation gradient $\mathbf{F}$ describes the transformation of the material point from the undeformed to the deformed configuration and is written in index notation as $F_{ij} = \partial x_i \big/ \partial X_j$ where $i, j = 1, 2, 3$. The left and the right Cauchy–Green deformation tensors which are given by $\mathbf{B} = \mathbf{F} \cdot \mathbf{F}^T$ and $\mathbf{C} = \mathbf{F}^T \cdot \mathbf{F}$, respectively, measure the geometric changes that occur due to deformation [40]. The polar decomposition theorem enables the decomposition of $\mathbf{F}$ into a product of pure rotation and symmetric positive-definite tensors as shown in Eq. (1).

$$\mathbf{F} = \mathbf{R} \cdot \mathbf{U} = \mathbf{V} \cdot \mathbf{R}, \tag{1}$$

where $\mathbf{R}$ is the orthogonal $\left(\mathbf{R}^{-1} = \mathbf{R}^T\right)$ rotation tensor whereas $\mathbf{U}$ and $\mathbf{V}$ are the right and left stretch tensors, respectively. Both $\mathbf{V}$ and $\mathbf{U}$ have the same eigenvalues but different eigenvectors as they are expressed in the deformed and undeformed configurations, respectively. The eigenvalues are principal stretches of the deformation and are denoted as λ_1, λ_2, and λ_3. From the principal stretches, the strain invariants of $\mathbf{B}$ and $\mathbf{C}$ are obtained as shown in Eq. (2):

$$\begin{aligned} I_1 &= \lambda_1^2 + \lambda_2^2 + \lambda_3^2, \\ I_2 &= \lambda_1^2\lambda_2^2 + \lambda_2^2\lambda_3^2 + \lambda_3^2\lambda_1^2, \\ I_3 &= \lambda_1^2\lambda_2^2\lambda_3^2. \end{aligned} \tag{2}$$

The determinant of $\mathbf{F}$, known as the Jacobian determinant $J = \det(\mathbf{F}) = \lambda_1\lambda_2\lambda_2 = \sqrt{I_3}$, describes the volume ratio V/V_0. A common assumption for elastomeric materials is that no volume change occurs during deformation, i.e., they are incompressible. This means that $J = I_3 = 1$. Consequently, an invariant-based phenomenological model with incompressibility assumption has W as a function of the first two invariants given in Eq. (2). While it has the advantage of simplifying the model equations, the assumption is an approximation of the material behavior. To capture the practical response, the W must include a volumetric term that is dependent on J. Compressibility consideration is highly significant particularly in hydrostatic deformations where volume changes range between 10 and 20% of the initial volume [41]. It is also important for the convergence of finite element simulations should the model be implemented in a finite element program. As such, formulations in this work will include the compressibility term.

To include a compressibility term in W expression, it is necessary to multiplicatively decompose $\mathbf{F}$ into dilatational and distortional components which are responsible for volume and shape changes, respectively. The relationship between dilatational and distortional parts of $\mathbf{F}$ and $\mathbf{B}$ is given in Eq. (3),

$$\begin{aligned} \mathbf{F} &= J^{(1/3)}\mathbf{F}^*, \\ \mathbf{B}^* &= \mathbf{F}^* \cdot \left(\mathbf{F}^*\right)^T = J^{(-2/3)}\mathbf{B}. \end{aligned} \tag{3}$$

The superscript * in Eq. (3) denotes the distortional part.

The W expression for a compressible model consists of two parts, one contributing to shape change and the other to volume change. The former is dependent on the distortional parts of the first two invariants which are obtained according to Eq. (4) whereas the latter is dependent on J:

$$\begin{aligned} I_1 &= J^{(2/3)} I_1^*, \\ I_2 &= J^{(4/3)} I_2^*. \end{aligned} \tag{4}$$

2.2 Cauchy stress tensor

A general invariant-based W expression with compressibility term is dependent on the first two invariants and the volume ratio $W = W(I_1, I_2, J)$. The first Piola–Kirchhoff stress tensor $\mathbf{P}$ is given as the partial derivative of W w.r.t each component of $\mathbf{F}$, $\mathbf{P} = \partial W/\partial F$. By applying the chain rule of differentiation, the general form of $\mathbf{P}$ is shown in Eq. (5),

$$\mathbf{P} = \frac{\partial W}{\partial I_1}\frac{\partial I_1}{\partial F} + \frac{\partial W}{\partial I_2}\frac{\partial I_2}{\partial F} + \frac{\partial W}{\partial J}\frac{\partial J}{\partial F}. \tag{5}$$

The relation between Cauchy stress tensor σ and $\mathbf{P}$ is given as $\sigma = (1/J)\mathbf{P}\mathbf{F}^T$. By substituting $\mathbf{P}$ with its expression given in Eq. (5), we obtain the general expression of the Cauchy stress tensor given in Eq. (6):

$$\sigma = \frac{1}{J}\left(\frac{\partial W}{\partial I_1}\frac{\partial I_1}{\partial F} + \frac{\partial W}{\partial I_2}\frac{\partial I_2}{\partial F} + \frac{\partial W}{\partial J}\frac{\partial J}{\partial F}\right)\mathbf{F}^T. \tag{6}$$

The derivatives of I_1, I_2, and J w.r.t $\mathbf{F}$ are given in Eq. (7),

$$\frac{\partial I_1}{\partial F} = 2\mathbf{F}, \quad \frac{\partial I_2}{\partial F} = 2I_1\mathbf{F} - 2\mathbf{F}\mathbf{F}^T\mathbf{F}, \quad \frac{\partial J}{\partial F} = J\mathbf{F}^{-T}. \tag{7}$$

Substituting the derivatives in Eq. (7) into Eq. (6), we obtain the σ expression given in Eq. (8),

$$\sigma = \frac{1}{J}\left(\frac{\partial W}{\partial I_1}2\mathbf{F}\mathbf{F}^T + \frac{\partial W}{\partial I_2}2I_1\mathbf{F}\mathbf{F}^T - \frac{\partial W}{\partial I_2}2\mathbf{F}\mathbf{F}^T\mathbf{F}\mathbf{F}^T + \frac{\partial W}{\partial J}J\mathbf{F}^{-T}\mathbf{F}^T\right). \tag{8}$$

Noting that $\mathbf{B} = \mathbf{F}\mathbf{F}^T$ and that $\mathbf{F}^{-\mathrm{T}}\mathbf{F}^{\mathrm{T}} = \mathbf{I}$, Eq. (8) can further be simplified to get the expression in Eq. (9),

$$\sigma = \frac{2}{J}\left(\frac{\partial W}{\partial I_1} + I_1\frac{\partial W}{\partial I_2}\right)\mathbf{B} - \frac{2}{J}\frac{\partial W}{\partial I_2}\mathbf{B}^2 + \frac{\partial W}{\partial J}\mathbf{I}, \tag{9}$$

where $\mathbf{I}$ is the identity tensor.

Again, W with compressibility assumption has to be written in terms of the volume ratio and distortional parts of the invariants as $W = W\left(I_1^*, I_2^*, J\right)$. For this reason, we substitute Eq. (4) into Eq. (9) and apply the chain rule of differentiation thus yielding the expression in Eq. (10),

$$\sigma = \frac{2}{J}\left(\frac{\partial W}{\partial I_1^*}\frac{\partial I_1^*}{\partial I_1} + J^{(2/3)} I_1^* \frac{\partial W}{\partial I_2^*}\frac{\partial I_2^*}{\partial I_2}\right)\mathbf{B} - \frac{2}{J}\frac{\partial W}{\partial I_2^*}\frac{\partial I_2^*}{\partial I_2}\mathbf{B}^2 + \left(\frac{\partial W}{\partial I_1^*}\frac{\partial I_1^*}{\partial J} + \frac{\partial W}{\partial I_2^*}\frac{\partial I_2^*}{\partial J} + \frac{\partial W}{\partial J}\right)\mathbf{I}. \tag{10}$$

Simplifying the expression in Eq. (10) requires the derivatives given in Eq. (11).

$$\begin{aligned} \frac{\partial I_1^*}{\partial I_1} &= J^{(-2/3)}, \ \frac{\partial I_1^*}{\partial J} = -\frac{2I_1^*}{3J}, \\ \frac{\partial I_2^*}{\partial I_2} &= J^{(-4/3)}, \ \frac{\partial I_2^*}{\partial J} = -\frac{4I_2^*}{3J}. \end{aligned} \tag{11}$$

Finally, substituting Eq. (11) into Eq. (10) and noting that $\mathbf{B}^* = J^{(-2/3)}\mathbf{B}$ yields the Cauchy stress tensor expression for arbitrary loading of elastomeric materials considering compressibility given in Eq. (12) [42],

$$\sigma = \frac{2}{J}\left(\frac{\partial W}{\partial I_1^*} + I_1^*\frac{\partial W}{\partial I_2^*}\right)\mathbf{B}^* - \frac{2}{J}\frac{\partial W}{\partial I_2^*}\left(\mathbf{B}^*\right)^2 + \left(\frac{\partial W}{\partial J} - \frac{2I_1^*}{3J}\frac{\partial W}{\partial I_1^*} - \frac{4I_2^*}{3J}\frac{\partial W}{\partial I_2^*}\right)\mathbf{I}. \tag{12}$$

As Eq. (12) is for arbitrary loading, the response in a specific loading mode is determined by **F**. The **F** expressions for each loading mode are given in Eq. (13),

$$\mathbf{F}_{\mathrm{UT}} = \begin{bmatrix} \lambda & 0 & 0 \\ 0 & \frac{1}{\sqrt{\lambda}} & 0 \\ 0 & 0 & \frac{1}{\sqrt{\lambda}} \end{bmatrix}, \ \mathbf{F}_{\mathrm{EB}} = \begin{bmatrix} \lambda & 0 & 0 \\ 0 & \lambda & 0 \\ 0 & 0 & \frac{1}{\lambda^2} \end{bmatrix}, \ \mathbf{F}_{\mathrm{PS}} = \begin{bmatrix} \lambda & 0 & 0 \\ 0 & 1 & 0 \\ 0 & 0 & \frac{1}{\lambda} \end{bmatrix}, \tag{13}$$

where the subscripts UT, EB, and PS represent uniaxial tension, equibiaxial extension, and pure shear, respectively.

3 Strain energy density functions

Many forms of W expressions including that of the Yeoh model emanate from the generalized Rivlin's model which is also known as the polynomial model. This Section introduces the polynomial model and two of the models that are derived from it.

3.1 Generalized Rivlin model

Rivlin and Saunders [43] proposed a form of W that is a double sum infinite power series of the first and the second invariants as shown in Eq. (14),

$$W = \sum_{i=0}^{N}\sum_{j=0}^{N} C_{ij}(I_1 - 3)^i (I_2 - 3)^j, \tag{14}$$

where C_{ij} are the model constants and $C_{00} = 0$ to obey the mathematical restriction that the strain energy should be zero at the unstrained state. If $N = 3$, then the terms of W are obtained as shown in Eq. (15),

$$\begin{aligned} W = {} & C_{10}(I_1-3) + C_{01}(I_2-3) + C_{11}(I_1-3)(I_2-3) + C_{20}(I_1-3)^2 + C_{02}(I_2-3)^2 + C_{21}(I_1-3)^2(I_2-3) \\ & + C_{12}(I_1-3)^1(I_2-3)^2 + C_{22}(I_1-3)^2(I_2-3)^2 + C_{30}(I_1-3)^3 + C_{03}(I_2-3)^3 + C_{31}(I_1-3)^3(I_2-3). \\ & + C_{13}(I_1-3)(I_2-3)^3 + C_{32}(I_1-3)^3(I_2-3)^2 + C_{23}(I_1-3)^2(I_2-3)^3 + C_{33}(I_1-3)^3(I_2-3)^3 \end{aligned} \tag{15}$$

This polynomial model is rarely used since obtaining the model constants is a complicated task especially at a large number of terms. Consequently, other forms of W are obtained by truncating the polynomial model to the first few terms. For instance, taking only the first term of Eq. (15) results in the neo-Hookean model $W = C_{10}(I_1 - 3)$ whereas taking the first two terms results in the Mooney–Rivlin model $W = C_{10}(I_1 - 3) + C_{01}(I_2 - 3)$. Of interest in this work are the forms of W obtained from Eq. (14) by neglecting the contribution of some terms. These are known as reduced polynomial models and are presented in the next Section.

3.2 Reduced polynomial models

As the merits of compressible hyperelastic models are already stated, we will include the volumetric term W_v (see Eq. (16)) in the W expressions. The term is most commonly used in the literature and meets the mathematical restrictions laid down for the volumetric part that includes $W_v(1) = 0,\ W_v^{'}(1) = 0,\ W_v^{''}(1) = K$ [44] to ensure that the strain energy and the stress are zero at the reference configuration and to ensure compatibility with the classical linear elasticity,

$$W_v = \frac{K}{2}(J-1)^2, \tag{16}$$

where K is the bulk modulus.

3.2.1 Biderman

Biderman [39] neglected the contribution of the terms containing $(I_2 - 3)$ except for the first term and considered the terms with $(I_1 - 3)$ to the third-order thus obtaining the W expression given in Eq. (17),

$$W = C_{10}\left(I_1^* - 3\right) + C_{20}\left(I_1^* - 3\right)^2 + C_{30}\left(I_1^* - 3\right)^3 + C_{01}\left(I_2^* - 3\right) + \frac{K}{2}(J-1)^2. \tag{17}$$

The derivatives necessary for obtaining the Cauchy stress tensor are given in Eq. (18):

$$\begin{aligned} \frac{\partial W}{\partial I_1^*} &= C_{10} + 2C_{20}\left(I_1^* - 3\right) + 3C_{30}\left(I_1^* - 3\right)^2, \\ \frac{\partial W}{\partial I_2^*} &= C_{01}, \\ \frac{\partial W}{\partial J} &= K(J-1). \end{aligned} \tag{18}$$

The Cauchy stress tensor expression for the Biderman model is obtained by substituting Eqs. (18) into Eq. (12) and is given by Eq. (19),

$$\begin{aligned} \sigma = &\frac{2}{J}\left[C_{10} + 2C_{20}\left(I_1^* - 3\right) + 3C_{30}\left(I_1^* - 3\right)^2 + I_1^* C_{01}\right]\mathbf{B}^* - \frac{2}{J}C_{01}\left(\mathbf{B}^*\right)^2 \\ &+ \left[K(J-1) - \frac{2I_1^*}{3J}\left(C_{10} + 2C_{20}\left(I_1^* - 3\right) + 3C_{30}\left(I_1^* - 3\right)^2\right) - \frac{4I_2^*}{3J}C_{01}\right]\mathbf{I}. \end{aligned} \tag{19}$$

3.2.2 Yeoh

Yeoh [9] completely neglected the contributions of the terms with $(I_2 - 3)$ and considered the $(I_1 - 3)$ terms up to the third order. From the general polynomial expression stated in Eq. (14), $j = 0$ and $N = 3$ resulting in the W expression for the Yeoh model as shown in Eq. (20):

$$W = C_{10}\left(I_1^* - 3\right) + C_{20}\left(I_1^* - 3\right)^2 + C_{30}\left(I_1^* - 3\right)^3 + \frac{K}{2}(J-1)^2. \tag{20}$$

The derivatives are given as:

$$\begin{aligned} \frac{\partial W}{\partial I_1^*} &= C_{10} + 2C_{20}\left(I_1^* - 3\right) + 3C_{30}\left(I_1^* - 3\right)^2, \\ \frac{\partial W}{\partial I_2^*} &= 0, \\ \frac{\partial W}{\partial J} &= K(J-1). \end{aligned} \tag{21}$$

Using Eq. (21) in Eq. (12) results in Yeoh's model Cauchy stress tensor expression for arbitrary loading as shown in Eq. (22),

$$\sigma = \frac{2}{J}\left[C_{10} + 2C_{20}\left(I_1^* - 3\right) + 3C_{30}\left(I_1^* - 3\right)^2\right]\mathbf{B}^* + \left[K(J-1) - \frac{2I_1^*}{3J}\left(C_{10} + 2C_{20}\left(I_1^* - 3\right) + 3C_{30}\left(I_1^* - 3\right)^2\right)\right]\mathbf{I}. \tag{22}$$

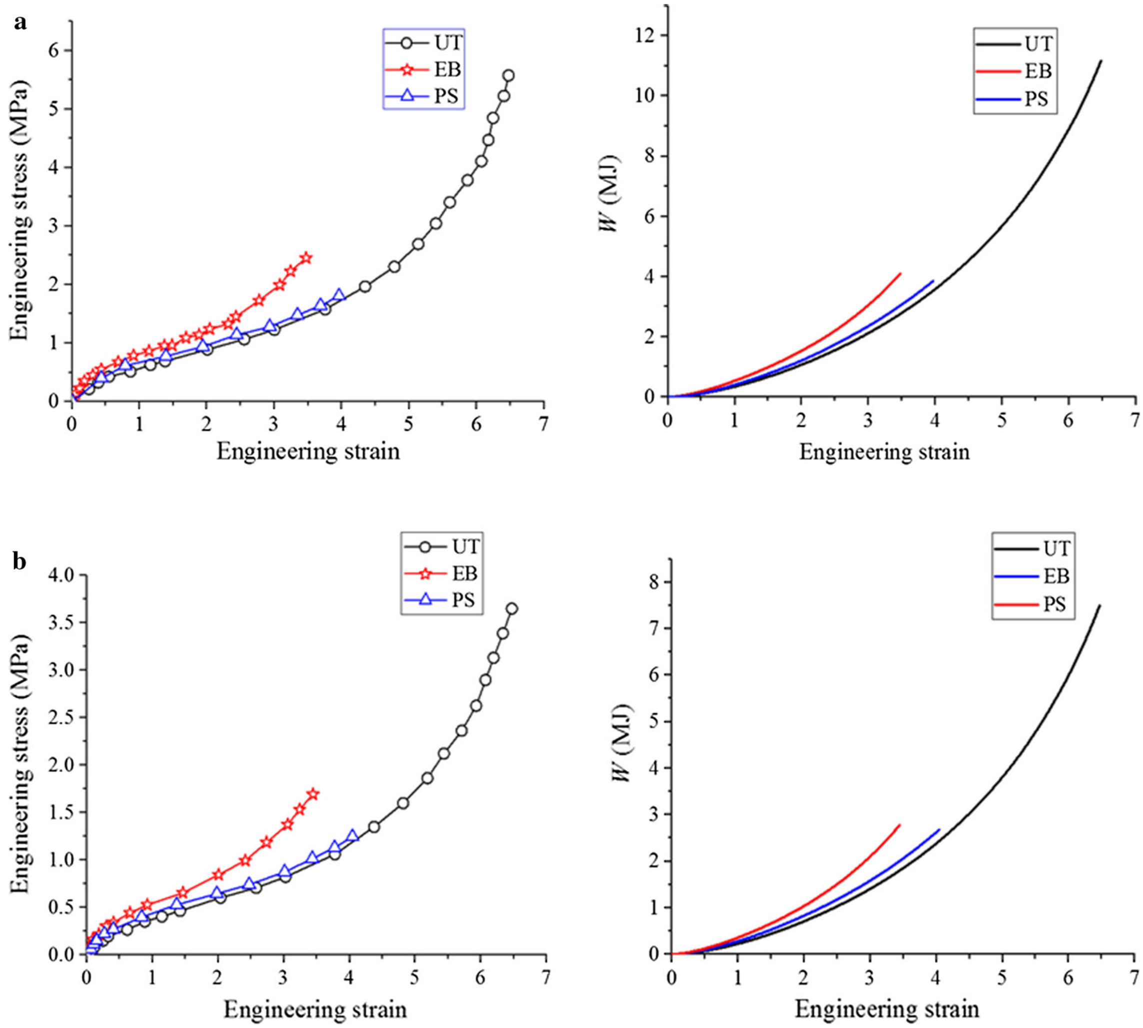

Fig. 1 The stress–strain and their corresponding W-strain plots of the experimental data utilized in this work. **a** The classical Treloar's [37] data for 8% S vulcanized rubber and **b** Zhao's [38] data for TPE

4 Model constants

The determination of model constants is the most important and delicate undertaking in phenomenological model development [45]. Establishing the model constants involves fitting the model's W expression to the strain energy/unit volume data which is obtained by calculating the area under the nominal stress–strain curve. While most models in the literature require data from different loading modes to be simultaneously fitted to get the best set of parameters, only data from the uniaxial tension loading are sufficient for our work. The relation between strain energy density and the strain is highly nonlinear and, therefore, nonlinear least-squares techniques are utilized for fitting and obtaining the model constants. The Levenberg–Marquardt algorithm (LMA) [46, 47] is the most popular nonlinear least-squares method for obtaining the model constants of hyperelastic models due to its robustness. This work utilizes the LMA method to determine the constants for the reduced polynomial models presented in Sect. 3.2.

As mentioned, two sets of experimental data from the literature were used. The first is the classical Treloar [37] data which has been the standard data in determining the predictability of new models whereas the second set of data was due to Zhao [38] which is of a TPE. The stress–strain plots of the experimental data and their corresponding W-strain plots are given in Fig. 1. From the stress–strain curves in Fig. 1, it is shown that the material undergoes large deformation particularly in the uniaxial tension loading (close to 700% engineering strains). The physical meaning of this behavior can be deduced by considering the microstructure of polymeric

Table 1 Model constants

Experimental data			
Model	Treloar [37] (8% S rubber)	Zhao [38] (TPE)	R^2
Biderman	$C_{10} = 144989.85,\ C_{20} = -551.50,$ $C_{30} = 29.94,\ C_{01} = 39734.81$	$C_{10} = 92364.74,\ C_{20} = -252.56,$ $C_{30} = 19.35,\ C_{01} = 32137.98$	0.9999
Yeoh	$C_{10} = 164907.76,\ C_{20} = -955.64,$ $C_{30} = 33.76$	$C_{10} = 108479.43,\ C_{20} = -579.83,$ $C_{30} = 22.45$	0.9999

materials. As put by Flory [48], polymeric materials exhibit high deformability and recoverability because their micro-molecular structure consists of long polymeric chains that are joined together into a three-dimensional network. Under an external load, the chains alter their arrangements and extensions. The large increase in stress at high deformation witnessed in the uniaxial tension stress–strain curves is due to the strain-induced crystallization which greatly increases the strength of the polymer. It is observed that the behavioral difference between the two materials is that TPE records lower stress levels.

The LMA was implemented in Python code. To determine how well the model was fitted, the coefficient of determination $\left(R^2\right)$ whose expression is given in Eq. (23) was employed to compare the predicted and the experimental data. It is worth noting that R^2 value close to unity implies a perfect fit,

$$R^2 = 1 - \frac{\sum_{i=1}^{n} (e_i - p_i)^2}{\sum_{i=1}^{n} (e_i - e_m)^2}. \tag{23}$$

The n, e_i, p_i, and e_m in Eq. (23) represent the number of data points, experimental data at a point i, predicted data at a point i, and the mean of the experimental data, respectively.

The model constants obtained are given in Table 1. The K values were obtained from literature as 1.5×10^9 and 1.2×10^9 for vulcanized rubber and TPE, respectively.

5 Model predictions

The predictions of the Biderman and Yeoh models presented in Sect. 3.2 were computed by implementing their Cauchy stress tensor expressions given in Eqs. (19) and (22), respectively, in Python codes. The code execution followed the algorithm given in Table 2.

The comparison of the model predictions with experimental data in the three loading modes for both vulcanized rubber and TPE is presented in this Section. As shown in Fig. 2a, both the Biderman and the Yeoh

Table 2 Algorithm for computing the model predictions in a Python code

User Input:

1. A vector of engineering strain
2. A vector of model constants

For all the engineering strain points, calculate:

i. The stretches
$\lambda = \varepsilon_{\text{eng}} + 1$

ii. Deformation gradients, $\mathbf{F}$, according to Eq. (13)

iii. The following:
$J = \det(\mathbf{F}), \mathbf{F}^* = J^{-1/3}\mathbf{F}, \mathbf{B}^* = J^{-2/3}\mathbf{B}, \mathbf{C}^* = J^{-2/3}\mathbf{C}, I_1^* = J^{-2/3}I_1, I_2^* = J^{-4/3}I_2$

iv. Cauchy stress tensor, σ, according to Eq. (19) and Eq. (22)

v. Von Mises stress from the components of the Cauchy stress tensor
$$\sigma_{\text{mises}} = \sqrt{\frac{1}{2}\left(\left(\sigma_{11} - \sigma_{22}\right)^2 + \left(\sigma_{22} - \sigma_{33}\right)^2 + \left(\sigma_{33} - \sigma_{11}\right)^2 + 6\left(\left(\sigma_{12}\right)^2 + \left(\sigma_{23}\right)^2 + \left(\sigma_{31}\right)^2\right)\right)}$$

vi. Engineering stress from the Cauchy stress
$$\sigma_{\text{eng}} = \frac{\sigma_{\text{true}}}{\varepsilon_{\text{eng}} + 1}$$

vii. Return σ_{eng}

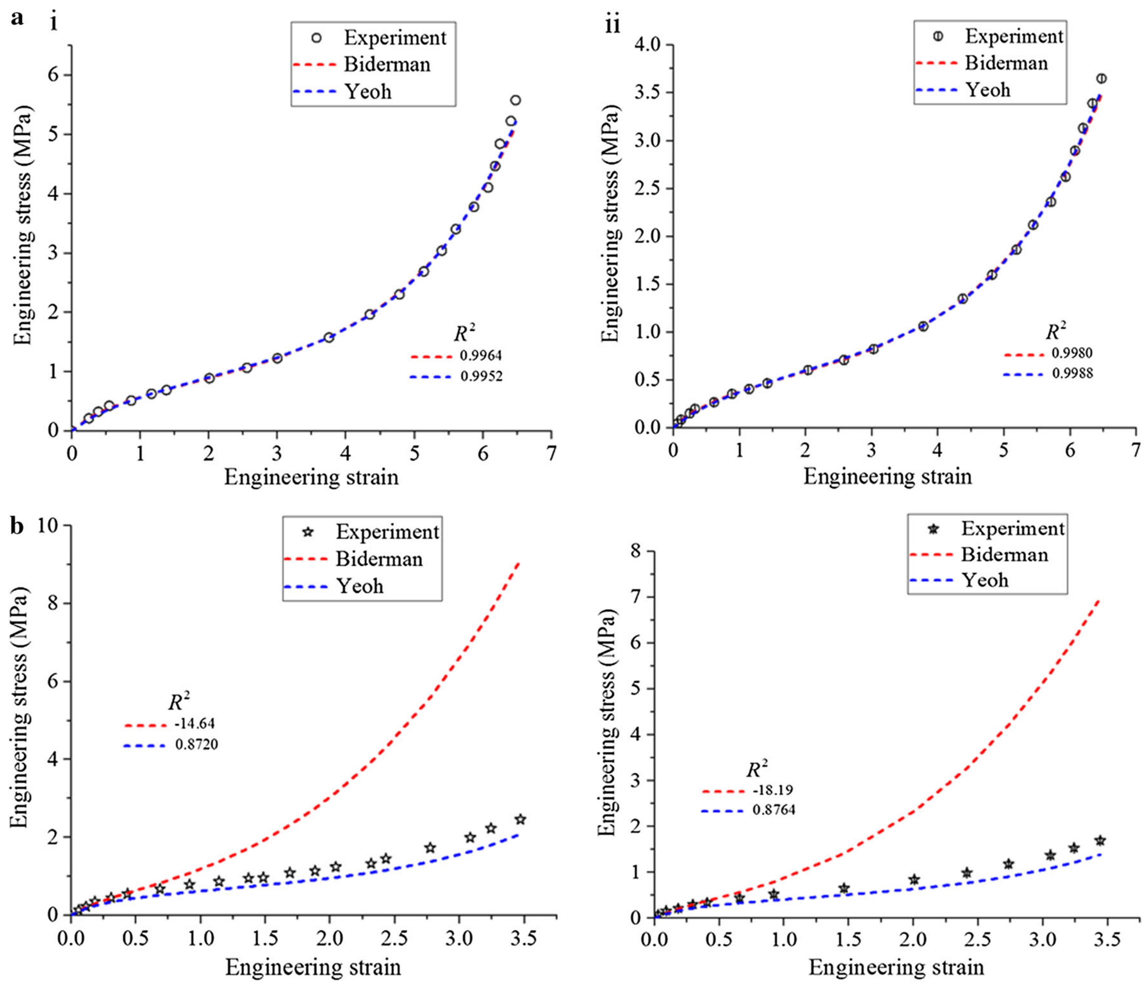

Fig. 2 Comparisons of the model predictions with experimental data for **a** uniaxial tension, and **b** equibiaxial tension loading. On the left (i) is Treloar's data for vulcanized rubber whereas on the right (ii) is Zhao's data for TPE

model predict the uniaxial tension behavior of vulcanized rubber and the TPE excellently with R^2 values of over 0.99. However, the behavior prediction in equibiaxial loading is of lower accuracy and highly distinctive between the two models. As shown in Fig. 2b, the Biderman model overestimates the stress which increases with strains leading to a negative R^2 of -14.64 and -18.19 for vulcanized rubber and TPE, respectively, meaning that the average of the predicted value highly deviates from the average values of the experimental data. On the other hand, Yeoh's model accuracy is acceptable for both materials as the R^2 value is about 0.87 even though it underestimates the stress.

In pure shear loading (see Fig. 3), both models predict excellently with R^2 values of over 0.96. The Biderman model performs better than the Yeoh model for both vulcanized rubber and TPE materials with the latter slightly underestimating the stress. These results show that the main challenge with the models is predicting equibiaxial tension behavior. Even though the Biderman model has a term containing the second invariant, its predictions in the said loading are far worse than those of the Yeoh model. The suggested modification to improve both models' prediction is proposed in the next Section.

6 Proposed modification

From the model predictions presented in the previous Section, it is demonstrated that the Biderman model performs excellently in predicting the uniaxial tension and pure shear loading but overestimates the stress in equibiaxial loading so much that the R^2 value is negative. On the other hand, the Yeoh model does well albeit

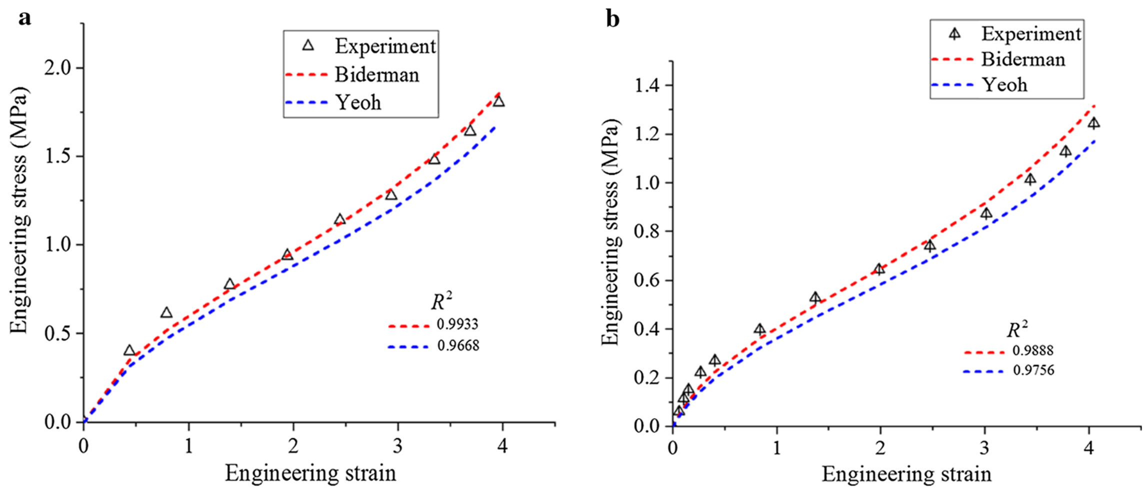

Fig. 3 Pure shear loading stress–strain plots of the model predictions and the experimental data for **a** vulcanized rubber and **b** TPE

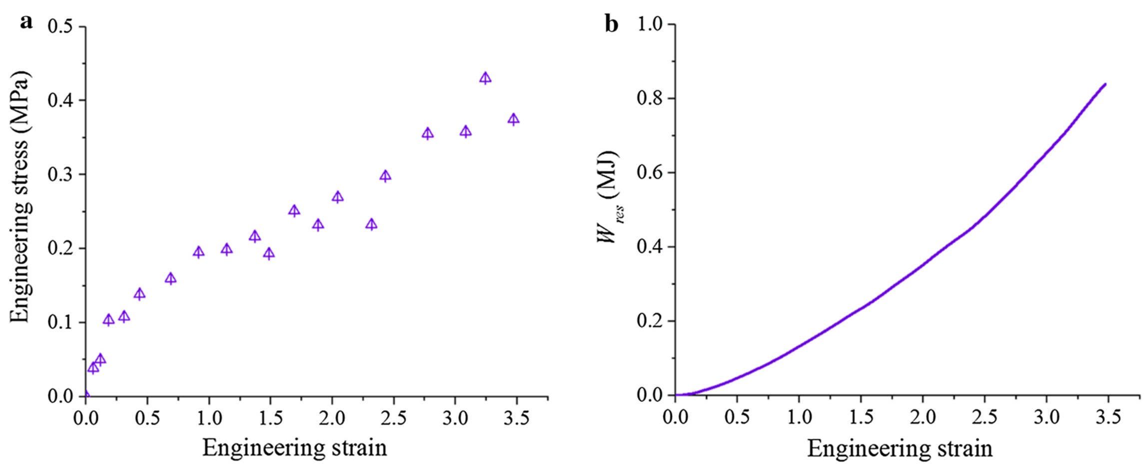

Fig. 4 The plots of **a** residual stress data points against the strain, and **b** the residual strain energy density against the strain

to relatively lower accuracy in equibiaxial loading as it underestimates the stress. The difference between the W expressions for Biderman and Yeoh models is that the former has an additional term containing the second invariant. In this Section, we propose the modification of Yeoh's W expression by adding a term that is dependent on the second invariant. It is the same as modifying the Biderman model by replacing the term containing the second invariant.

Inspired by Carroll's [14] systematic method of obtaining the W expression, we start by noting that the residual stress in equibiaxial loading is highly significant. If σ_{eb} is the experimental stress data for equibiaxial extension loading and σ_{pred} is the predicted data of the same loading by the Yeoh model, then the residual stress is given by $\sigma_{\text{res}} = \sigma_{\text{eb}} - \sigma_{\text{pred}}$. The second step is to calculate the strain energy density of the residual stress W_{res} (the area under the residual stress–strain curve). The plots of the residual stress data points and the strain energy density against the strain are given in Fig. 4.

The third and the most important step is the fitting of the residual strain energy density plotted in Fig. 4b into a term that is dependent on the second invariant. After a rigorous fitting process, the expression in Eq. (24) was found to perfectly fit the residual strain energy data with R^2 value of 0.9961 as shown in Fig. 5.

$$W_{res} = D\left(\sqrt{I_2} - \sqrt{3}\right) \tag{24}$$

where D is the model constant.

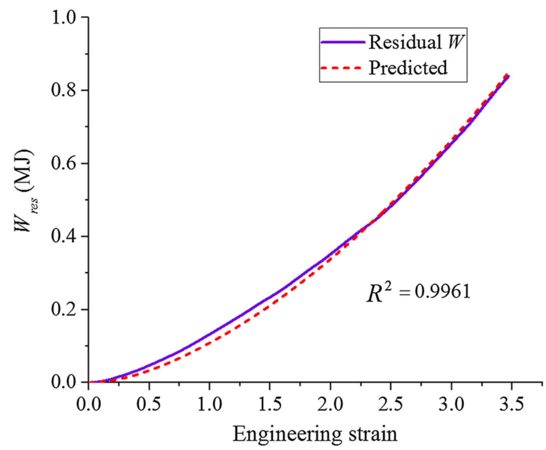

Fig. 5 Comparison of the calculated and predicted residual strain energy density

Table 3 Constants for the modified Yeoh model

Experimental data	Constants	R^2
Treloar [37]	$C_{10} = 150725.24$, $C_{20} = -592.34$, $C_{30} = 30.17$, $D = 117771.78$	0.9999
Zhao [38]	$C_{10} = 97083.51$, $C_{20} = -287.64$, $C_{30} = 19.56$, $D = 94592.19$	0.9999

Having obtained the term that describes the residual strain energy density, the next step is to add the term to the original Yeoh model W expression given in Eq. (20) to obtain the modified version shown in Eq. (25),

$$W = C_{10}\left(I_1^* - 3\right) + C_{20}\left(I_1^* - 3\right)^2 + C_{30}\left(I_1^* - 3\right)^3 + D\left(\sqrt{I_2^*} - \sqrt{3}\right) + \frac{K}{2}(J-1)^2, \tag{25}$$

where C_{10}, C_{20}, C_{30}, and D are the model constants. The derivatives of Eq. (25) w.r.t I_1^*, I_2^*, and J are given in Eq. (26),

$$\begin{aligned} \frac{\partial W}{\partial I_1^*} &= C_{10} + 2C_{20}\left(I_1^* - 3\right) + 3C_{30}\left(I_1^* - 3\right)^2, \\ \frac{\partial W}{\partial I_2^*} &= \frac{D}{2\sqrt{I_2^*}}, \\ \frac{\partial W}{\partial J} &= K(J-1). \end{aligned} \tag{26}$$

By substituting the derivatives in Eq. (26) into Eq. (12), we obtain the modified Yeoh's model Cauchy stress tensor expression (see Eq. (27)) for arbitrary loading of elastomeric materials,

$$\begin{aligned} \sigma = \frac{2}{J}&\left[C_{10} + 2C_{20}\left(I_1^* - 3\right) + 3C_{30}\left(I_1^* - 3\right)^2 + \frac{I_1^* D}{2\sqrt{I_2^*}}\right]\mathbf{B}^* - \frac{D}{J\sqrt{I_2^*}}\left(\mathbf{B}^*\right)^2 \\ &+ \left[K(J-1) - \frac{2I_1^*}{3J}\left(C_{10} + 2C_{20}\left(I_1^* - 3\right) + 3C_{30}\left(I_1^* - 3\right)^2\right) - \frac{2I_2^*}{3J}\frac{D}{\sqrt{I_2^*}}\right]\mathbf{I} \end{aligned}. \tag{27}$$

The model constants for the modified version given in Table 3 were obtained by fitting its W expression given in Eq. (25) to the uniaxial tension data of the two sets of experimental data used for this work.

7 Results and discussion

The performances of the original and the modified Yeoh model (this work) in reproducing the experimental data for 8% S vulcanized rubber and thermoplastic elastomer (TPE) obtained from Treloar [37] and Zhao [38],

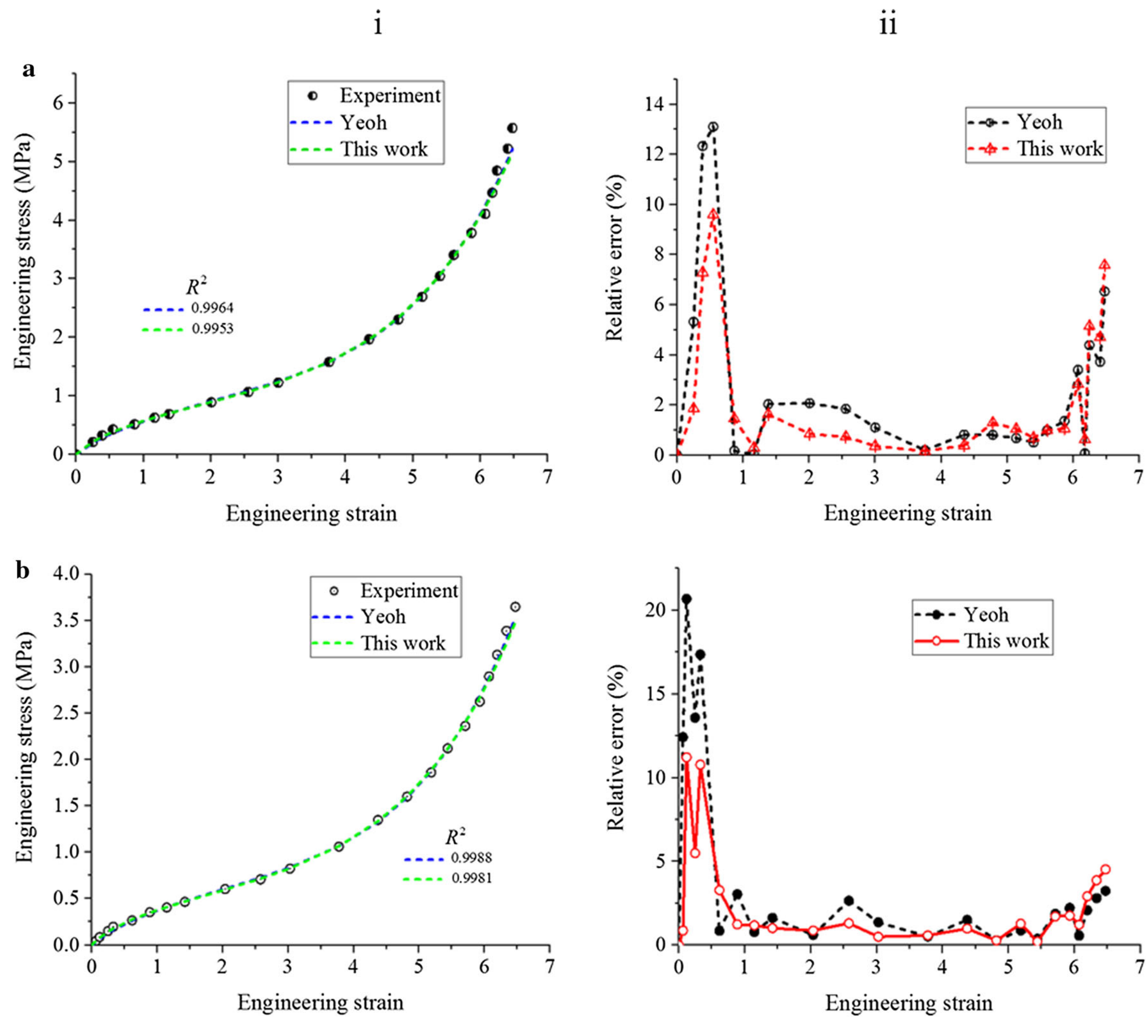

Fig. 6 Comparisons of the uniaxial tension experimental data and model predictions and their corresponding plots of percentage relative error in each data point for **a** 8% S vulcanized rubber and **b** TPE

respectively, are presented. Apart from the coefficient of determination R^2 given in Eq. (23), the percentage relative error δ, whose expression is given in Eq. (28), is also used to quantify the predictive capabilities of the models. After presenting the engineering stress–strain plots for each loading mode accompanied by their corresponding R^2 values and δ-strain plots, the overall behavior for each model is presented (the average of R^2 and δ) as

$$\delta = \left(\frac{|\sigma_{\text{exp}} - \sigma_{\text{pred}}|}{\sigma_{\text{exp}}} \right) \times 100 \tag{28}$$

where σ_{exp} and σ_{pred} are the experimental and model-predicted stresses, respectively.

7.1 Uniaxial tension

The models exhibited excellent and comparable predictions in uniaxial tension loading mode. As shown in Fig. 6 (a, i) and (b, i), the models reproduced the experimental data accurately with R^2 values of over 0.99, and their similar behavior makes it difficult to differentiate the curves. However, the plots of percentage relative error in each strain data point as shown in Fig. 6(a, ii) and (b, ii) demonstrate that this work's model records lower relative errors.

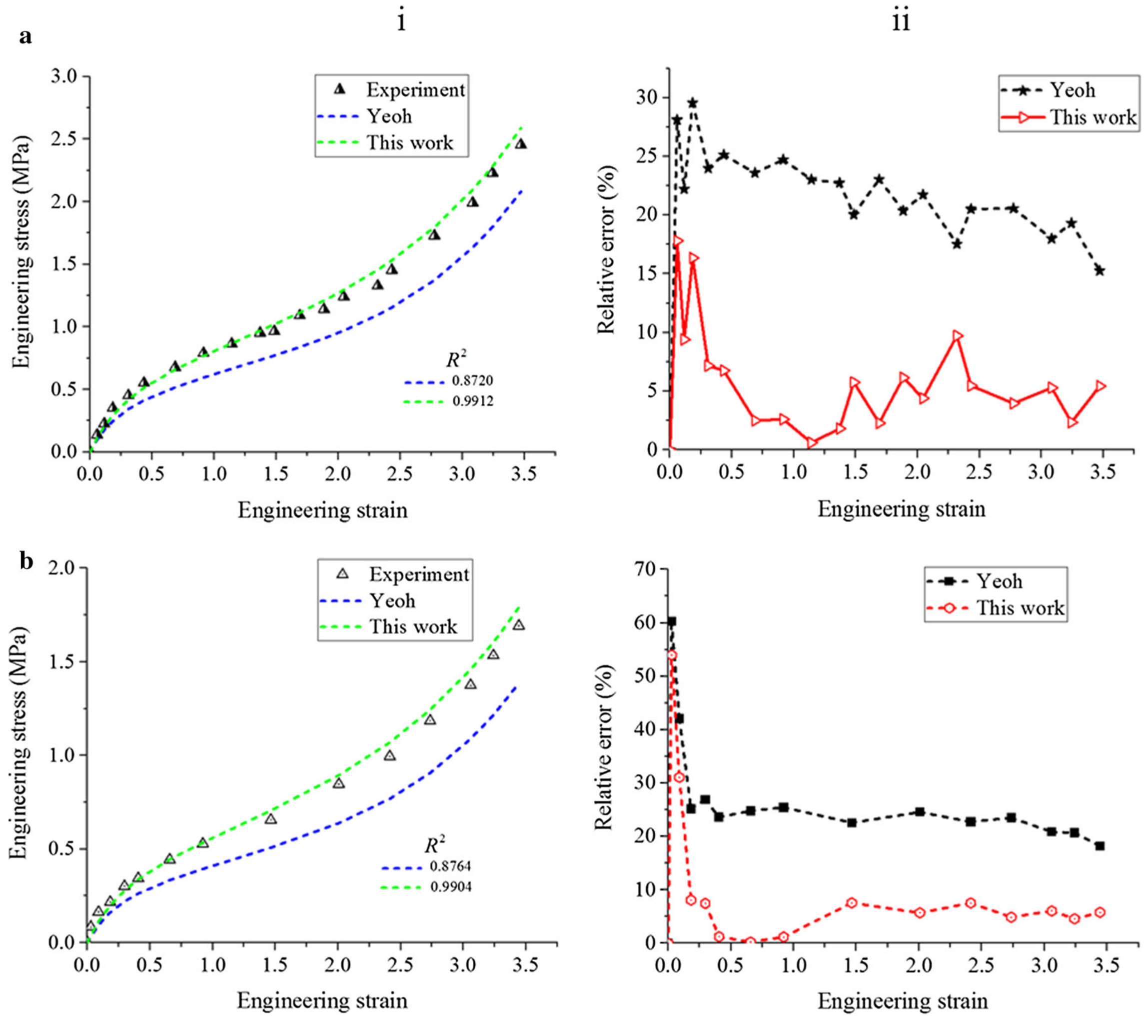

Fig. 7 Comparisons of model predictions and experimental data for equibiaxial extension loading and their corresponding plots of percentage relative error for **a** 8% vulcanized rubber and **b** TPE

7.2 Equibiaxial extension

Remarkable improvements in equibiaxial extension loading predictive capabilities were demonstrated by this work's model. As shown in Fig. 7(a, i) and (b, i) for 8% vulcanized rubber and TPE, respectively, the Yeoh model underestimates the stress leading to a relatively lower R^2 value of 0.87 whereas this work's model accurately describes the behavior with R^2 value of 0.99. The percentage relative error plots in Fig. 7(a, ii) and (b, ii) further illustrate more clearly the predictive superiority of this work's model. The Yeoh model is shown to record higher relative errors as opposed to this work's model.

7.3 Pure shear

By observation of the stress–strain plots shown in Fig. 8(a, i) and (b, i), it is shown that both Yeoh and this work's model posted accurate predictions in pure shear loading. The predictions are comparable though this work's model is slightly more accurate with R^2 value of 0.98 compared to 0.96 for the Yeoh model. According to the relative error plots given in Fig. 8 (a, ii) and (b, ii), the advantage of this work's model is evident as it recorded relatively lower errors.

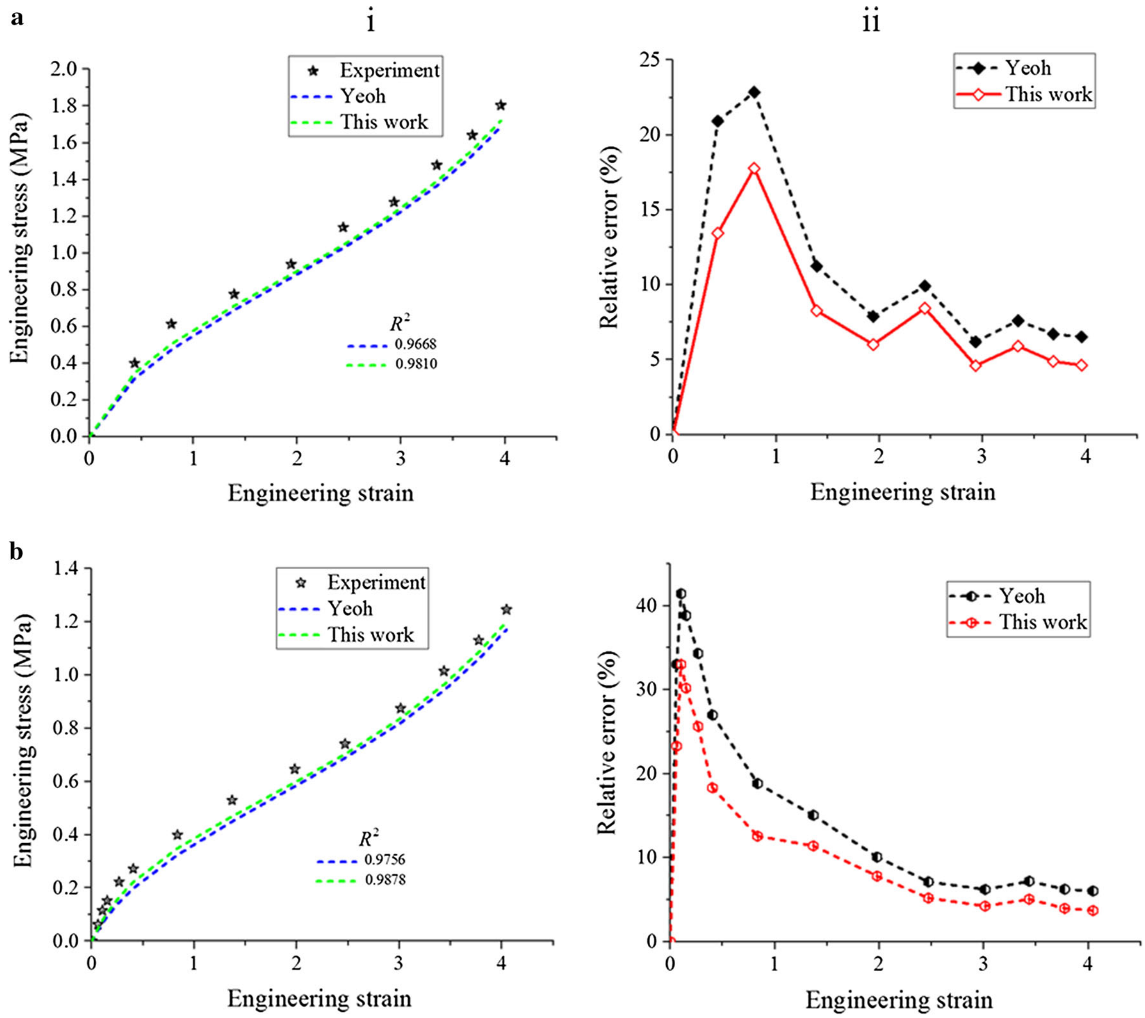

Fig. 8 The engineering stress–strain plots of model predictions and experimental data in pure shear loading and their corresponding relative error-strain plots for **a** 8% vulcanized rubber and **b** TPE

7.4 Overall behavior

As the practical loads on elastomeric components are complex and involve multi-axial loading conditions, it is crucial to understand the *overall behavior* of the model in predicting the mechanical response. In this case, the *overall behavior* signifies the capability of the model to accurately describe the response in the case of multi-axial loading. To quantify this, the average R^2 and δ values for the three loading modes are obtained for each model.

The average relative errors in each loading mode are presented in Fig. 9, wherein this work's model is shown to record significantly lower errors particularly in the equibiaxial loading mode. The errors in uniaxial tension predictions are completely acceptable (both models were found to reproduce this loading mode excellently) as they are below 5%. This work's model performs better particularly in Zhao's data where the average error is 2.59% compared to Yeoh's model 4.153%. The predictive strength of this work's model is demonstrated in its ability to accurately describe the equibiaxial loading thereby reducing average relative errors from 22.07 to 6.09 and from 27.25 to 10.29% for data due to Treloar and Zhao, respectively.

For each model, the overall R^2 and relative error values were obtained by an average of the values in each loading mode. As shown in Fig. 10a, this work's model exhibits an excellent overall behavior with an overall R^2 of 0.99 as opposed to Yeoh's model 0.94. The overall behavior in terms of the relative errors is shown in Fig. 10b where the errors recorded by the Yeoh model are roughly twice those of this work's model.

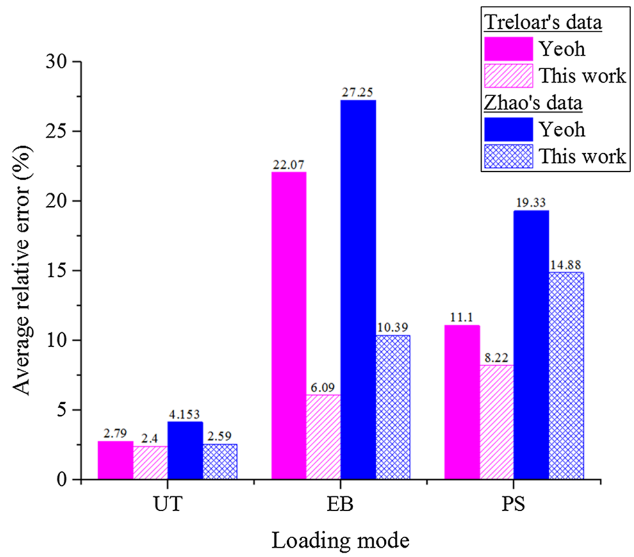

Fig. 9 The average relative errors in each loading mode for data due to Treloar [37] (8% vulcanized rubber) and Zhao [38] (TPE)

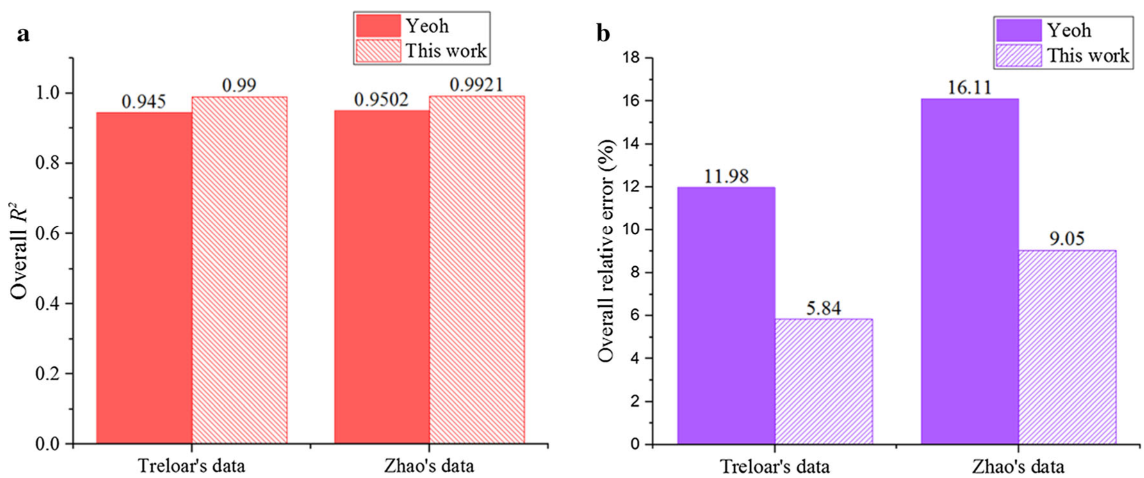

Fig. 10 The models' overall **a** R^2 and **b** percentage relative error

The improvement in the predictive capabilities is attributed to the inclusion of the term containing the second invariant in the W expression of the Yeoh model.

8 Conclusions

A hyperelastic model that can be utilized to reliably describe the mechanical response of engineering components under practical loading conditions should be able to accurately reproduce the experimental data in uniaxial tension, equibiaxial extension, and pure shear loading modes. Furthermore, the models formulated via the phenomenological approach should require a single set of model constants that are obtained by fitting the model's W expression to experimental data from a single loading mode, e.g., uniaxial tension.

The relatively lower predictive performance of the Yeoh model in the equibiaxial loading mode is attributed to the lack of dependence on the second invariant in its W expression. The overall performance of the Yeoh model in the case of multi-axial loading conditions can be improved by adding a term containing the second invariant to its original W expression. The difference between the W expressions for the Yeoh and the Biderman models is that the latter has an additional term containing the second invariant. However, the Biderman model overestimates the stress in the equibiaxial mode so much that the coefficient of determination yields a negative value. As such, the addition of the term with the second invariant should follow a specific method.

This work has demonstrated that notable improvements, particularly in the equibiaxial loading mode, are achieved when a systematic approach is followed in determining the form of the term with the second invariant. The residual stress in equibiaxial loading (the difference between the experimental and the Yeoh model predicted stress) is highly significant. The residual strain energy density is calculated (the area under the residual stress–strain curve) and fitted to a term that is dependent on the second invariant. Finally, the term is added to the original W expression resulting in a modified version. The Cauchy stress tensor equations derived from the W expressions were implemented in Python codes, and the performance of the original and the modified versions were compared based on two sets of experimental data obtained from the literature, the classical data of 8% S vulcanized rubber and the recent data of a thermoplastic elastomer. The two different sets of experimental data were chosen purposely to test the models' capabilities to predict the behavior of different materials.

The modification led to excellent predictive capabilities in all the loading modes. For instance, the relative errors in the modified version's equibiaxial tension loading predictions were just a third of those for the original version. Overall, the relative errors for the modified version were half as many as for the original version. Thus, the modified version is highly suitable for the accurate prediction of the multi-axial loading behavior of elastomeric materials. While the accuracy in predictions for vulcanized rubber and thermoplastic elastomer was comparable, the latter posted comparatively higher relative errors. Future work should focus on checking the suitability of the modified model to more elastomeric materials and soft tissues.

Funding This work was supported by the National Natural Science Foundation of China (Grant Nos. 11632005 and 11672086).

Availability of data and material Data available upon request from the corresponding author.

Declarations

Conflict of interest All authors certify that they have no affiliations with or involvement in any organization or entity with any financial interest or non-financial interest in the subject matter or materials discussed in this manuscript.

References

1. Yuan, L., Gu, Z.-X., Yin, Z.-N., Xiao, H.: New compressible hyper-elastic models for rubberlike materials. Acta Mech. **226**, 4059–4072 (2015)
2. Mooney, M.: A theory of large elastic deformation. J. Appl. Phys. **11**(9), 582–592 (1940)
3. Muhr, A.H.: Modeling the stress–strain behavior of rubber. Rubber Chem. Technol. **78**(3), 391–425 (2005)
4. Yeoh, O.H., Fleming, P.D.: A new attempt to reconcile the statistical and phenomenological theories of rubber elasticity. J. Polym. Sci.: Part B: Polym. Phys. **35**(12), 1919–1931 (1997)
5. Bahreman, M., Darijani, H., Fooladi, M.: Constitutive modeling of isotropic hyperelastic materials using proposed phenomenological models in terms of strain invariants. Polym. Eng. Sci. **56**(3), 299–308 (2016)
6. Treloar, L.R.G.: The Physics of Rubber Elasticity, 3rd edn. Oxford University Press, Oxford (1975)
7. Rivlin, R.S.: Large elastic deformations of isotropic materials. IV. Further developments of the general theory. Phil. Trans. R. Soc. Lond. A **241**, 379–397 (1948)
8. Yeoh, O.H.: Some forms of the strain energy function for rubber. Rubber Chem. Technol. **66**(5), 754–771 (1993)
9. Yeoh, O.H.: Characterization of elastic properties of carbon-black-filled rubber vulcanizates. Rubber Chem. Technol. **63**(5), 792–805 (1990)
10. Ogden, R.W.: Large deformation isotropic elasticity—on the correlation of theory and experiment for incompressible rubberlike solids. Proc. R. Soc. Lond. A **326**(1567), 565–584 (1972)
11. Gent, A.N.: A new constitutive relation for rubber. Rubber Chem. Technol. **69**(1), 59–61 (1996)
12. Arruda, E.M., Boyce, M.C.: A three-dimensional constitutive model for the large stretch behavior of rubber elastic materials. J. Mech. Phys. Solids **4**(2), 389–412 (1993)
13. Kaliske, M., Heinrich, G.: An extended tube-model for rubber elasticity: statistical-mechanical theory and finite element implementation. Rubber Chem. Technol. **72**(4), 602–632 (1999)
14. Carroll, M.M.: A strain energy function for vulcanized rubbers. J. Elasticity **103**, 173–187 (2011)
15. Anssari-Benam, A., Bucchi, A.: A generalised neo-Hookean strain energy function for application to the finite deformation of elastomers. Int. J. Non-Linear Mech. **128**, 103626 (2021)
16. Yaya, K., Bechir, H.: A new hyper-elastic model for predicting multi-axial behaviour of rubber-like materials: formulation and computational aspects. Mech. Time-Dependent Mater. **22**, 167–186 (2018)
17. Mansouri, M.R., Darijani, H.: Constitutive modeling of isotropic hyperelastic materials in an exponential framework using a self-contained approach. Int. J. Solids Struct. **51**, 4316–4326 (2014)

18. Khajehsaeid, H., Arghavani, J., Naghdabadi, R.: A hyperelastic constitutive model for rubber-like materials. Eur. J. Mech. A/Solids **38**, 144–151 (2013)
19. Zhao, Z., Mu, X., Du, F.: Modeling and verification of a new hyperelastic model for rubber-like materials. Math. Probl. Eng. **2019**, 2832059 (2019)
20. Bien-Aimé, L.K.M., Blaise, B.B., Beda, T.: Characterization of hyperelastic deformation behavior of rubber-like materials. SN Appl. Sci. **2**, 648 (2020)
21. Külcü, İD.: A hyperelastic constitutive model for rubber-like materials. Arch. Appl. Mech. **90**, 615–622 (2020)
22. Marckmann, G., Verron, E.: Comparison of hyperelastic models for rubber-like materials. Rubber Chem. Technol. **79**(5), 835–858 (2006)
23. Fujikawa, M., Maeda, N., Yamabe, J., Koishi, M.: Performance evaluation of hyperelastic models for carbon-black–filled SBR vulcanizates. Rubber Chem. Technol. **93**(1), 142–156 (2020)
24. Seibert, D.J., Schöche, N.: Direct comparison of some recent rubber elasticity models. Rubber Chem. Technol. **73**(2), 366–384 (2000)
25. Hossain, M., Amin, A.F.M.S., Kabir, M.N.: Eight-chain and full-network models and their modified versions for rubber hyperelasticity: a comparative study. J. Mech. Behav. Mater. **24**(1–2), 11–24 (2015)
26. Hohenberger, T.W., Windslow, R.J., Pugno, N.M., Busfield, J.J.C.: A constitutive model for both low and high strain nonlinearities in highly filled elastomers and implementation with user-defined material subroutines in Abaqus. Rubber Chem. Technol. **92**(4), 653–686 (2019)
27. Melly, S.K., Liu, L., Liu, Y., Leng, J.: Improved Carroll's hyperelastic model considering compressibility and its finite element implementation. Acta. Mech. Sin. **37**, 785–796 (2021)
28. Xiao, H.: An explicit, direct approach to obtaining multiaxial elastic potentials that exactly match data of four benchmark tests for rubbery materials—part 1: incompressible deformations. Acta Mech. **223**, 2039–2063 (2012)
29. Yu, L., Jin, T., Yin, Z., Xiao, H.: A model for rubberlike elasticity up to failure. Acta Mech. **226**, 1445–1456 (2015)
30. Cao, J., Ding, X.-F., Yin, Z.-N., Xiao, H.: Large elastic deformations of soft solids up to failure: new hyperelastic models with error estimation. Acta Mech. **228**, 1165–1175 (2017)
31. Gajewski, M., Szczerba, R., Jemioło, S.: Modelling of elastomeric bearings with application of Yeoh hyperelastic material model. Procedia Eng. **111**, 220–227 (2015)
32. Renaud, C., Cros, J.-M., Feng, Z.-Q., Yang, B.: The Yeoh model applied to the modeling of large deformation contact/impact problems. Int. J. Impact Eng. **36**, 659–666 (2009)
33. Jaramillo, H.E.: Evaluation of the use of the Yeoh and Mooney-Rivlin functions as strain energy density functions for the ground substance material of the annulus fibrosus. Math. Probl. Eng. **2018**, 1570142 (2018)
34. Forsat, M.: Investigating nonlinear vibrations of higher-order hyper-elastic beams using the Hamiltonian method. Acta Mech. **231**, 125–138 (2020)
35. Horgan, C.O., Saccomandi, G.: Simple torsion of isotropic, hyperelastic, incompressible materials with limiting chain extensibility. J. Elast. **56**, 159–170 (1999)
36. Horgan, C.O., Smayda, M.G.: The importance of the second strain invariant in the constitutive modeling of elastomers and soft biomaterials. Mech. Mater. **51**, 43–52 (2012)
37. Treloar, L.R.G.: Stress-strain data for vulcanized rubber under various types of deformation. Rubber Chem. Technol. **17**(4), 813–825 (1944)
38. Zhao, F.: Continuum constitutive modeling for isotropic hyperelastic materials. Adv. Pure Math. **6**, 571–582 (2016)
39. Biderman, V.L.: Calculation of rubber parts. Rascheti na prochnost **40** (1958) (**in Russian**)
40. Reddy, J.N.: An Introduction to Continuum Mechanics, 2nd edn. Cambridge University Press, Cambridge (2013)
41. Bischoff, J.E., Arruda, E.M., Grosh, K.: A new constitutive model for the compressibility of elastomers at finite deformations. Rubber Chem. Technol. **74**(4), 541–559 (2001)
42. Bergström, J.: Mechanics of Solid Polymers: Theory and Computational Modeling. William Andrew, New York (2015)
43. Rivlin, R.S., Saunders, D.W.: Large elastic deformations of isotropic materials VII. Experiments on the deformation of rubber. Philos. Trans. R. Soc. Lond. Ser. A, Math. Phys. Sci. **243**(865), 251–288 (1951)
44. Horgan, C.O., Murphy, J.G.: On the volumetric part of strain-energy functions used in the constitutive modeling of slightly compressible solid rubbers. Int. J. Solids Struct. **46**, 3078–3085 (2009)
45. Ogden, R.W., Saccomandi, G., Sgura, I.: Fitting hyperelastic models to experimental data. Comput. Mech. **34**, 484–502 (2004)
46. Levenberg, K.: A method for the solution of certain non-linear problems in least squares. Q. Appl. Math. **2**(2), 164–168 (1944)
47. Marquardt, D.W.: An algorithm for least-squares estimation of nonlinear parameters. J. Soc. Ind. Appl. Math. **11**(2), 431–441 (1963)
48. Flory, P.J.: Molecular theory of rubber elasticity. Polym. J. **17**(1), 1–12 (1985)